



## Full Length Article

# Microstructure, mechanical and tribological characterization of CrN/DLC/Cr-DLC multilayer coating with improved adhesive wear resistance

Xudong Sui<sup>a,b,\*</sup>, Jinyu Liu<sup>a,c</sup>, Shuaituo Zhang<sup>a,b</sup>, Jun Yang<sup>a</sup>, Junying Hao<sup>a,\*</sup>

<sup>a</sup>State Key Laboratory of Solid Lubrication, Lanzhou Institute of Chemical Physics, Chinese Academy of Science, Lanzhou 730000, China

<sup>b</sup>Qingdao Center of Resource Chemistry and New Materials, Qingdao 266000, China

<sup>c</sup>University of Chinese Academy of Sciences, Beijing 100049, China

## ARTICLE INFO

## Article history:

Received 15 September 2017

Revised 27 November 2017

Accepted 30 December 2017

Available online 6 January 2018

## Keywords:

Multilayer coatings

CrN

DLC

Friction and wear

Adhesive wear

## ABSTRACT

Adhesive wear is one of the major reasons for the failure of components during various tribological application, especially for rubbing with viscous materials. This study presents CrN/DLC/Cr-DLC multilayer composite coatings prepared on a plasma enhanced chemical vapor deposition (PECVD) device with the close field unbalanced magnetron sputtering ion plating (CFUBMSIP) technique. SEM, XRD and Raman spectroscopy were used to determine the structure of multilayer coatings. It was found that the multilayer coatings are composed by the alternating CrN and DLC layers. Compared with the single CrN coatings, the friction coefficient of the CrN/DLC/Cr-DLC multilayer coating decreases about more than seven times after sliding a distance of 500 m. This helps to reduce the adhesive wear of multilayer coatings. Compared with the single CrN and DLC coating, the wear rate of the CrN/DLC/Cr-DLC multilayer coating is reduced by an order of magnitude to  $7.10 \times 10^{-17}$  (sliding with AISI 440C) and  $2.64 \times 10^{-17}$  (sliding with TC4)  $\text{m}^3/(\text{N m})$ . The improved tribological performance of multilayer coatings mainly attributes to the introduction of lubricant DLC and hard support CrN layers, the enhancement of crack propagation inhibition, and the increment of elastic recovery value  $W_e$  (71.49%) by multilayer design method.

© 2018 Elsevier B.V. All rights reserved.

## 1. Introduction

Adhesive wear is one of the major reasons for the failure of components during various tribological applications, such as forming, cutting, sliding and so on [1–3]. The adhesion bonds can degrade the friction environment and significantly increase the frictional heat, especially for rubbing with viscous materials. In turn, excessive frictional heat will facilitate the formation of the adhesion bonding. These adhesive bonds shear off eventually and take away part of coating materials. The results is increased wear, deteriorated surface quality and poor machining accuracy [4–6]. Therefore, the intensive adhesive wear has become one of the most critical challenges for various friction applications and needs to be solved.

Nowadays, a variety of vapor deposition coatings are used to reduce wear [7–10]. Among them, the transition metal nitrides, such as TiN, CrN and TiAlN, are the most popular coatings for their high hardness, excellent oxidation resistance and thermal stability

[11–13]. Recently, there have been continuous efforts to further improve tribological performance of these coatings by using element doping, architecture design and also new deposition technology, including closed field unbalanced magnetron sputter ion plating (CFUBMSIP), high power impulse magnetron sputtering (HiPIMS) and so on [14,15]. However, transition metal nitride coating itself can not lubricate the rubbing pairs effectively, which leads to excessive friction and adhesive wear. Thus, adaptive lubricious coating and polished post-treatment were developed to solve this problem [16–18]. Many studies have shown that a decrease in the friction coefficient can reduce the adhesive wear effectively [18]. However, although the friction coefficient of the transition metal nitride coating can be partially reduced by these methods, it still does not meet the growing demands for wear resistance in modern tribological application, and the post-treatment process also increases the cost. Thus, it is necessary to propose an improvement coating material with a low friction coefficient in order to solve these issues. Recently, diamond-like carbon (DLC) films have attracted an increasing interest in various lubrication environments owing to their low friction coefficient and good chemical inertness [19–21]. These excellent properties make the DLC coating suitable for using in the field of anti-wear. However, there are some imperfection restricting their industrial applications, such

\* Corresponding authors at: State Key Laboratory of Solid Lubrication, Lanzhou Institute of Chemical Physics, Chinese Academy of Science, Lanzhou 730000, China (X. Sui).

E-mail addresses: [suixudong@licp.cas.cn](mailto:suixudong@licp.cas.cn) (X. Sui), [jyhao@licp.cas.cn](mailto:jyhao@licp.cas.cn) (J. Hao).

as poor oxidation resistance, low thermal stability and high intrinsic compressive stress [19,22]. Thus it can be seen that the advantages and disadvantages of transition metal nitride and DLC coatings maybe complement each other. It would be of much interest to make a composite coating consisting of both transition metal nitride and DLC coatings.

Recently, multilayer design has drawn much attention in hard coating industry, which plays an important role in obtaining the optimal mechanical and tribological properties of both layers materials. A variety of ceramic/metal, metal/metal and ceramic/ceramic multilayered coatings, such as TiN/Ti, Cu/Cr, TiAlN/CrN, etc., have been intensively studied [23–26]. However, the multilayer coatings consisting of transition metal nitride and DLC have not been well studied [27,28]. Therefore, with the question of how the tribological properties of transition metal nitride coatings are improved when DLC coatings are introduced through multilayer design method, we successfully deposited the CrN/DLC/Cr-DLC multilayer coating. The microstructures as well as mechanical and tribological properties of a multilayer CrN/DLC/Cr-DLC, the single CrN and the single DLC coatings were studied in this work. A reduction in friction and wear of the CrN/DLC/Cr-DLC multilayer composite coating could be obtained through multilayer design.

## 2. Experimental section

### 2.1. Sample preparation

The CrN/DLC/Cr-DLC multilayer composite coatings were deposited on commercial n-type Si (100) wafer and AISI 440C steel ( $\Phi$  25 mm  $\times$  4 mm,  $R_a \leq 0.05 \mu\text{m}$ ) substrates using a commercial PECVD machine with CFUBMSIP technique. For comparison, the single CrN and DLC coatings were also prepared. The substrates were sequentially cleaned with acetone and alcohol for 10 min in an ultrasonic cleaner before deposition. The chamber was evacuated to a background vacuum below  $1.0 \times 10^{-3}$  Pa, and then the substrates were Ar ion etched for 30 min at a pulsed bias voltage of  $-400$  V (frequency: 250 kHz, pulsewidth: 500 nsec). Afterwards, Cr layer with a thickness of about 150 nm was deposited as the intermediate layer. Then the CrN layers and DLC layers were prepared by alternately triggering or turning off C or Cr targets and opening or closing  $\text{N}_2$  or  $\text{C}_4\text{H}_{10}$  pipe. In this process, the CrN layer and DLC layer were applied with a pulsed voltage of  $-100$  V and  $-75$  V respectively. Finally, a top layer of Cr-DLC was deposited on the surface of multilayer coatings with a pulsed voltage of  $-75$  V. The detailed experimental parameters are listed in Table 1.

### 2.2. Coating characterization

The morphologies and thickness of the coatings were characterized by scanning electron microscope (SEM, Hitachi S-4800). An energy dispersive spectrometer (EDS, Oxford) was used for evaluating the chemical composition. The crystal structure of the

coatings was analysed by X-ray diffraction (XRD, Shimadzu 6100) with Cu  $K\alpha$  radiation ( $\lambda = 1.540598$  nm, 40 kV, 30 mA). The Raman signals were detected by a spectrometer (Horiba, LabRam HR Evolution) with an excitation wavelength of 532 nm at a resolution of  $2 \text{ cm}^{-1}$ .

The hardness and elastic modulus were performed by using a nanoindenter (Agilent, Nano Indenter XP) with a Berkovich diamond tip. The maximum indentation depth was controlled at about 15% of the coating thickness. Each sample was tested 5 times in order to obtain mean values of hardness and elastic modulus. The adhesion force were tested on a multi-functional tester for materials surface properties (MFT-4001). The fracture toughness was evaluated by indentation method on a Vickers hardness tester (Future-tech, FM-800) under a load of 300 g. The tribological behaviours of the coatings were evaluated by a ball-on-disk tribometer (CSM, TRB) in an ambient atmosphere. The disk was the coated steel substrate. The counterpart was AISI 440C steel ball ( $\Phi$ 3 mm, HRC  $\sim$  60,  $R_a \sim 0.10 \mu\text{m}$ ) of 8 mm in diameter. The tests were carried out at the normal load of 3 N, line speed of 10 cm/s and the fixed sliding distance was 500 m. After the tribological tests, morphology and composition of the wear tracks were investigated by SEM and 3D non-contact surface profiler (Kla-Tencor, Micro-XAM800). The wear rate  $k$  was given by the Eq. (1) [29]:

$$k = V/SN \quad (1)$$

where  $V$  is the wear volume;  $S$  is the total sliding distance;  $N$  is the normal load.

## 3. Results and discussion

### 3.1. Structure and morphology

The EDS results of the different coatings are listed in Table 2. Although the hydrogen has not been detected by EDX technique, it is almost certain that the existence of hydrogen in the DLC or Cr-DLC coatings derived from  $\text{C}_4\text{H}_{10}$  source gas plasmas. Cross-section morphologies of the coatings were observed by SEM as shown in Fig. 1. The deposited coatings are dense and uniform. All the coatings have a Cr buffer layer of about 150 nm and the thicknesses of our coatings ranged from about 1.25 to  $2.0 \mu\text{m}$ . In addition, a CrC intermediate layer is added in the single DLC coatings to strengthen the adhesion force between coatings and sub-

**Table 2**  
EDS results of the different coatings.

Point	Cr (at.%)	C (at.%)	N (at.%)
A	6.73	93.27	–
B	27.89	72.11	–
C	48.47	–	51.53
D	22.11	77.89	–
E	17.54	82.46	–

**Table 1**  
Deposition parameters for the coatings.

Coatings	CrN/DLC/Cr-DLC				CrN		DLC		
	Cr	CrN	DLC	Cr-DLC	Cr	CrN	Cr	CrC	DLC
Cr target power (DC, A)	4	4	–	2	4	4	4	4 $\rightarrow$ 0	–
C target power (RF, W)	–	–	350	–	–	–	–	–	350
Bias voltage (V)	$-100$	$-100$	$-75$	$-75$	$-100$	$-100$	$-100$	$-75$	$-100$
Pressure (Pa)	2	2.5	3 $\rightarrow$ 4	4.2	2	2.5	2	2 $\rightarrow$ 4	4
Ar flow rate (sccm)	35	35	35	35	35	35	35	35	35
$\text{N}_2$ flow rate (sccm)	–	25	–	–	–	25	–	–	–
$\text{C}_4\text{H}_{10}$ flow rate (sccm)	–	–	8 $\rightarrow$ 15	15	–	–	–	4 $\rightarrow$ 15	15
Deposition time (s)	600	650 * 10	350 * 9	800	600	5200	600	2160	7200

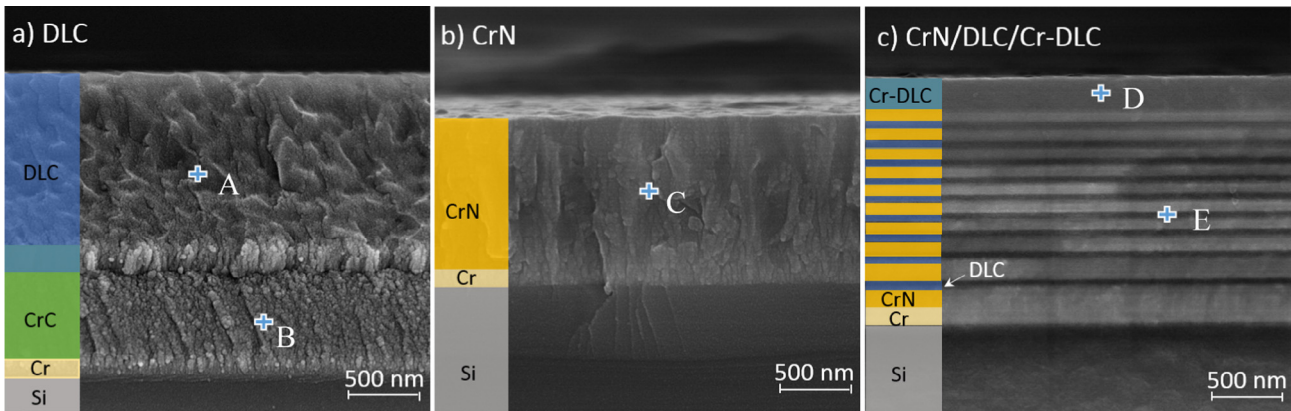


Fig. 1. Cross-section SEM images of the coatings: (a) DLC, (b) CrN, and (c) CrN/DLC/Cr-DLC.

strates. A typical structure of CrN/DLC/Cr-DLC multilayer coating is presented in Fig. 1c, containing the alternating coatings of CrN layers (120 nm) and DLC layers (53 nm), and the top layer Cr-DLC layer (236 nm). It can be found that the interface between the multilayers is tightly bonded and no significant peeling occurs.

The XRD patterns of the CrN and CrN/DLC/Cr-DLC multilayer coatings are shown in Fig. 2. The hollow triangle and dot in Fig. 2 represents the diffraction peaks of AISI 440C substrate and Cr inter-

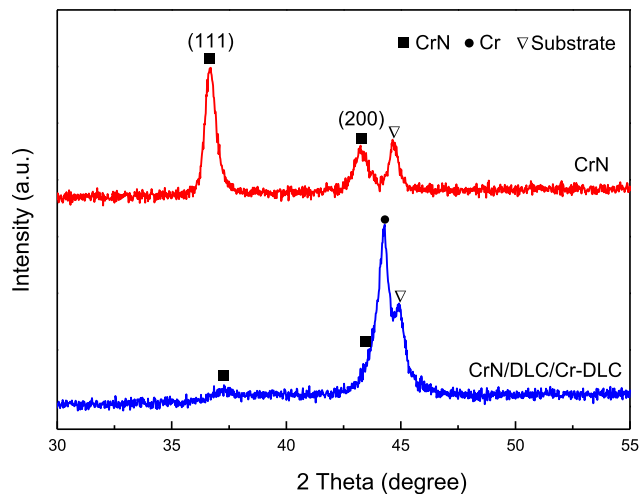


Fig. 2. XRD pattern of the single CrN and multilayer CrN/DLC/Cr-DLC coatings.

layer, respectively. The solid square represents the standard XRD patterns of fcc structure CrN. It can be found that the CrN and CrN/DLC/Cr-DLC multilayer coatings all contains fcc CrN phase. And there is no obvious diffraction peaks about carbon in the multilayer coating. Therefore, the carbon should be presented with an amorphous form in the multilayer coating.

To better characterize the microstructure of the coatings, the atomic bond structure of DLC and CrN/DLC/Cr-DLC coatings was studied by Raman analysis as shown in Fig. 3. Generally, the Raman spectra of the coatings in the range of  $800\text{--}2000\text{ cm}^{-1}$  can be fitted to two Gaussian peaks (D peak and G peak). The D peak is attributed to the breathing mode of  $\text{sp}^2$  atoms in rings at around  $1350\text{ cm}^{-1}$ , and G peak derives from the stretching vibration symmetry of pair of  $\text{sp}^2$  carbon atoms in aromatic rings or chains located at around  $1580\text{ cm}^{-1}$  [30]. According to the results of Raman spectrum, the intensity ratio of D peak to G peak ( $I_D/I_G$ ), full width at half maximum of G peak ( $G_{FWHM}$ ) and G peak position can be obtained. These information is closely related to the structure of the carbon based coatings. As shown in Fig. 3, the  $I_D/I_G$  value of the CrN/DLC/Cr-DLC multilayer coating increases from 0.72 to 1.55 compared with the single DLC coating. In addition, compared with the single DLC coating, the G peak position of the CrN/DLC/Cr-DLC multilayer coating shifts upward from  $1532.68\text{ cm}^{-1}$  to  $1544.37\text{ cm}^{-1}$  and  $G_{FWHM}$  decreases from  $179.78\text{ cm}^{-1}$  to  $152.89\text{ cm}^{-1}$ . All these changes imply the CrN/DLC/Cr-DLC multilayer coating owns a reduced  $\text{sp}^3$  (C–C) to  $\text{sp}^2$  (C=C) ratio. This is mainly caused by the incorporation of Cr into the amorphous carbon matrix by multilayer design. Since the incorporation of Cr element can result in

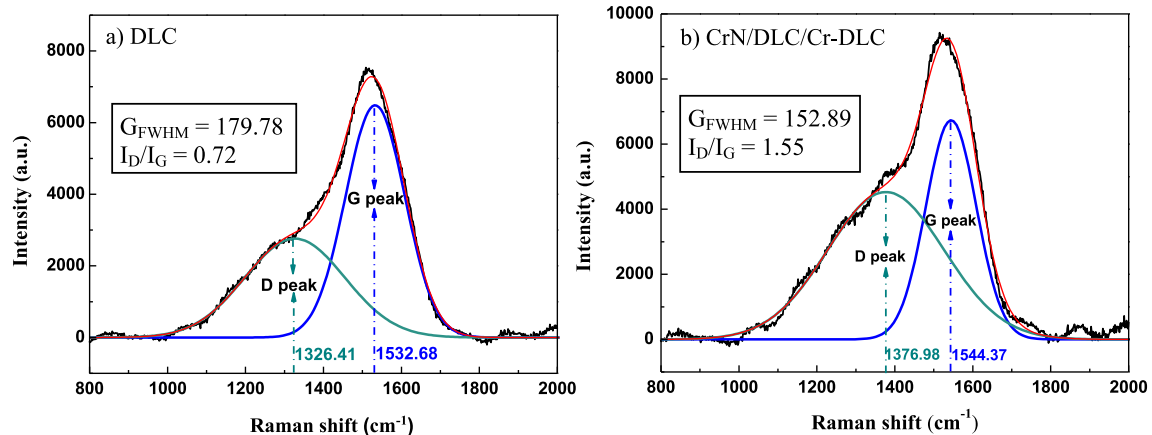


Fig. 3. Raman spectra of the coatings: (a) the single DLC and (b) the multilayer CrN/DLC/Cr-DLC.

structural ordering and promote the formation of C=C bonds organized in delocalized rings, then a higher degree of graphite-like character were obtained in the CrN/DLC/Cr-DLC multilayer coating [31].

### 3.2. Mechanical and tribological properties

The nanoindentation test is often used to characterize the hardness of coatings. Fig. 4a show the nanoindentation test results of the prepared coatings. It can be found that the single CrN coatings have the highest hardness of about 26 GPa, which is due to the dense coating structure prepared by CFUBMSIP technique and the nature feature of the transition metal nitride. However, in this work, the hardness of the CrN/DLC/Cr-DLC multilayer coatings is lower than that of the single DLC coatings. Generally, the  $sp^3$  bonding are strongly combined with covalent bond for enhancing the hardness of DLC coatings [32–34]. Thus, the decrease in hardness of the multilayer coatings may be owing to a reduced fraction of  $sp^3$  bonding observed by Raman analysis.

In addition, the elastic recovery value ( $W_e$ ) can be derived from the typical load–displacement curves shown in Fig. 4b. The elastic recovery value ( $W_e$ ), defined as  $[(d_{\max} - d_{\text{res}})/d_{\max}] \times 100\%$ , where  $d_{\max}$  is the maximum indentation depth during loading and  $d_{\text{res}}$  is the residual indentation depth after unloading. The  $W_e$  value stands for the elasticity recovery capacity, which can reflect the toughness of the sample to some extent [35,36]. For the single coatings, the  $W_e$  value of the DLC and CrN coating is 54.26% and 66.81% respectively, which implies the elastic or reversible defor-

mation is predominant during indentation process. Compared with the single DLC coating, the  $W_e$  value of the CrN/DLC/Cr-DLC coating rises from 54.26% to 71.49%, indicating an increase in the toughness of the multilayer coating.

To better characterize the fracture toughness of the coatings, a Vickers hardness tester has been used to conduct an indentation experiments on above coatings with a load of 300 g. The indentation morphologies are presented in Fig. 5. It can be observed that the indentation morphology of DLC coating (Fig. 5b) shows large radial cracks and delaminated regions, revealing a poor fracture toughness. The single CrN coating (Fig. 5a) shows a large amount of transverse cracks in and around the indentation. This is mainly due to the high hardness and brittle of nitride coatings. However, the CrN/DLC/Cr-DLC multilayer coating (Fig. 5c) presents the best indentation morphology. The indentation morphology of CrN/DLC/Cr-DLC coating is clear and free of any large cracks. The interface effect caused by multilayer design can suppress crack propagation in the coatings. Moreover, according to the previous reports, the decrease of  $sp^3$  content in multilayer coating can lead to a relatively low hardness, which can also help increasing the coating toughness [36].

Adhesion strength is also important to the friction application of the coatings, especially for the cutting industry. The adhesion strength was tested by a scratch tester under a progressive normal load. When the tip scratches the coating surface, the friction force between tip and coating is recorded as shown in Fig. 6. It can be observed that the friction force first increase linearly with the loading force, which means the coating did not delaminate from the

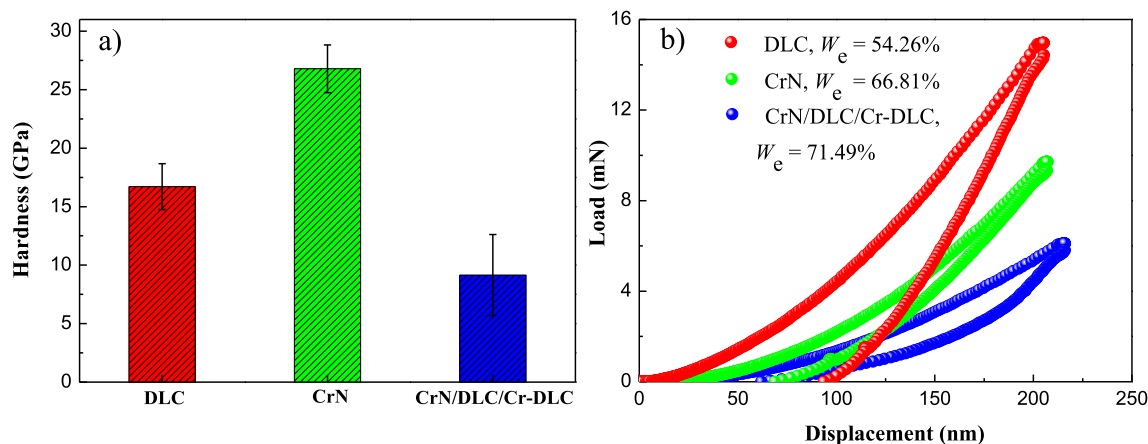


Fig. 4. (a) Nanoindentation test results of different coatings and (b) typical loading–unloading curves during indentation test.

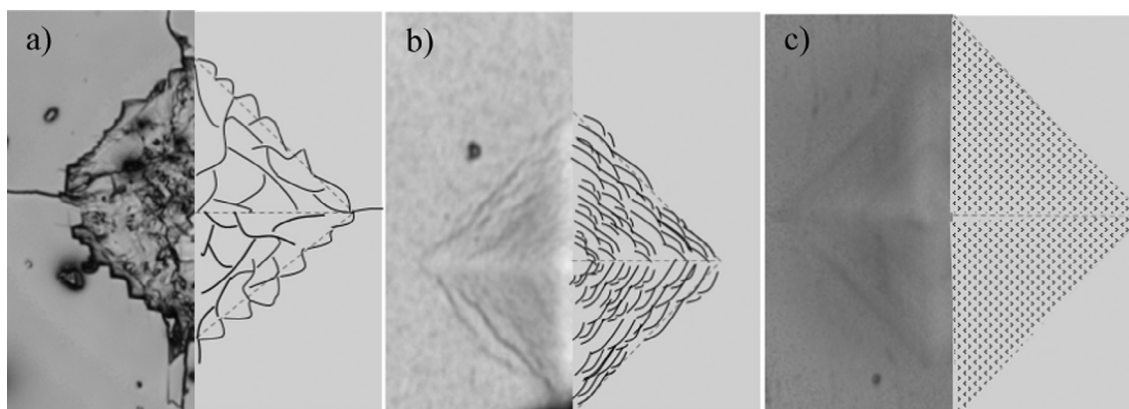


Fig. 5. Indentation morphologies of different coatings: (a) DLC, (b) CrN, and (c) CrN/DLC/Cr-DLC.



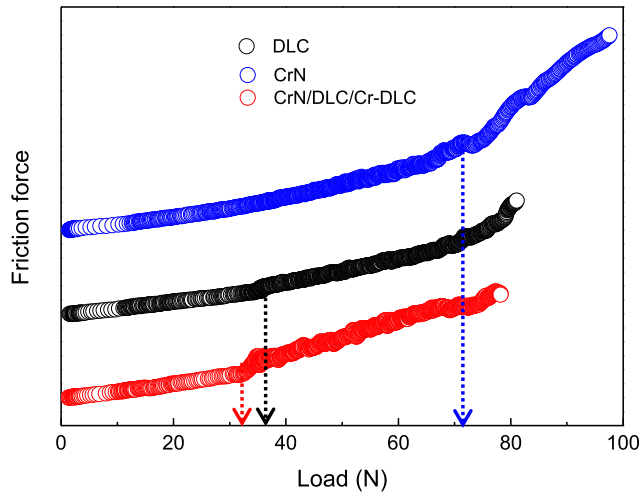


Fig. 6. Friction force curves of coatings during the scratch test.

substrates. When continue to increase normal load, the friction force may have an abrupt change (shown by the arrow in Fig. 6), which reveals the occurrence of delamination and adhesion failure. The normal load at this time can be used to characterize the adhesion force of the coatings. Using this method, it can be observed that the CrN coating has the highest adhesion force of about 70 N. This can satisfy various tribological applications including cutting, forming, etc. The adhesion force of DLC and CrN/DLC/Cr-DLC coatings is about 30–35 N. This can meet the common tribological applications under low load. However, there is a need to further increase the adhesion strength for meeting the demand of high load tribological applications.

In order to study the adhesive wear resistance of the coatings, two different viscous materials were selected as friction pairs. The friction coefficient results are shown in Fig. 7. The friction coefficient between coating and titanium alloy is less than that with 440C stainless steel. The single CrN coating has the highest friction coefficient of about 0.861 (sliding against AISI 440C ball) and 0.599 (sliding against TC4 ball). Compared with the single CrN coating, the friction coefficient of CrN/DLC/Cr-DLC coating decreases about more than seven times to 0.112 after sliding against AISI 440C, which is close to the friction coefficient of DLC coating. When the friction pair becomes a more viscous titanium alloy, the friction coefficient of CrN/DLC/Cr-DLC coating can obtain a lowest value of 0.087. Thus, it can be concluded that the CrN/DLC/Cr-DLC composite coating could reach a stable low friction coefficient after a

long sliding against AISI440C or TC4 ball of about 500 m. The low friction coefficient of multilayer coating can be attributed to the introduction of lubricant amorphous carbon based layers [37].

To better characterize the coating tribological behaviour, the 3D optical profile images of wear tracks were studied as shown in Fig. 8. When the friction pair is 440C stainless steel, the wear track of the DLC coating is smooth and little wear debris is found alongside the wear track. In contrast, the wear track of CrN coating is wider and rougher. There exists a lot of adhesive bonds on the wear track of CrN coating, which implies an intensive adhesive wear occurs during the friction test. This difference can be easily observed from the cross sectional profile of wear tracks in Fig. 8. For the CrN/DLC/Cr-DLC multilayer coating, its wear track shows a unique appearance different from both CrN and DLC coating. The wear track in the middle of the multilayer coating is smooth and little debris, which is similar to that of the DLC coating. And there is a small amount of adhesive bonds on the edges of the wear track, which is similar to the wear morphology of the CrN coating. The change of wear track morphology of the multilayer coatings is mainly affected by its low friction coefficient, which can make the viscous materials not easy to bond with the coating.

When the friction pair changes to TC4 titanium alloy, the wear track of the DLC coating is still smooth and clear. The wear depth decreases from 380 to 135 nm due to the decrease of the friction coefficient between coatings and titanium ball. However, the CrN coating suffers from more severe wear after sliding against titanium ball. The wear depth and adhesions are all increased. This is mainly due to the high reactivity between titanium and nitride coating. These adhesive bonds shears off eventually and takes away part of coating materials during the rubbing process. As a result, the coating is severely worn. Fortunately, despite a slightly increased amount of adhesive bonds, the wear tracks of the CrN/DLC/Cr-DLC multilayer coating remains clear and small. Therefore, through the multilayer design, the adhesive resistance and tribological properties can be improved.

Fig. 9 shows the calculated wear rates of the deposited coatings. With sliding against AISI 440C ball, the wear rates of the single CrN and DLC coating are  $3.76 \times 10^{-16}$  and  $8.91 \times 10^{-16} \text{ m}^3/(\text{N m})$ , respectively. It is worth noting that the wear rate of CrN/DLC/Cr-DLC composite coating can be reduced by an order of magnitude to  $7.10 \times 10^{-17} \text{ m}^3/(\text{N m})$  through the multilayer design method. When the friction pair changes to TC4 ball, the wear rate of the DLC and CrN/DLC/Cr-DLC coatings is further reduced to  $8.81 \times 10^{-17}$  and  $2.64 \times 10^{-17} \text{ m}^3/(\text{N m})$  respectively. In contrast, the wear rate of the CrN coating increases significantly. Since the CrN coating is too worn, it cannot calculate the wear rate by volume from 3D images of the wear tracks. The approximate wear rate of

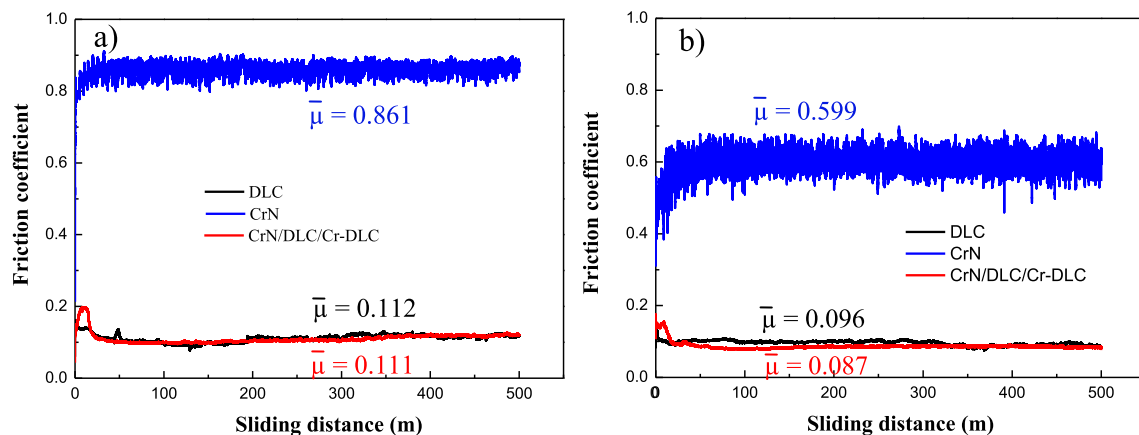


Fig. 7. Friction coefficient of the coatings with different friction pair: (a) AISI 440C ball and (b) TC4 ball.

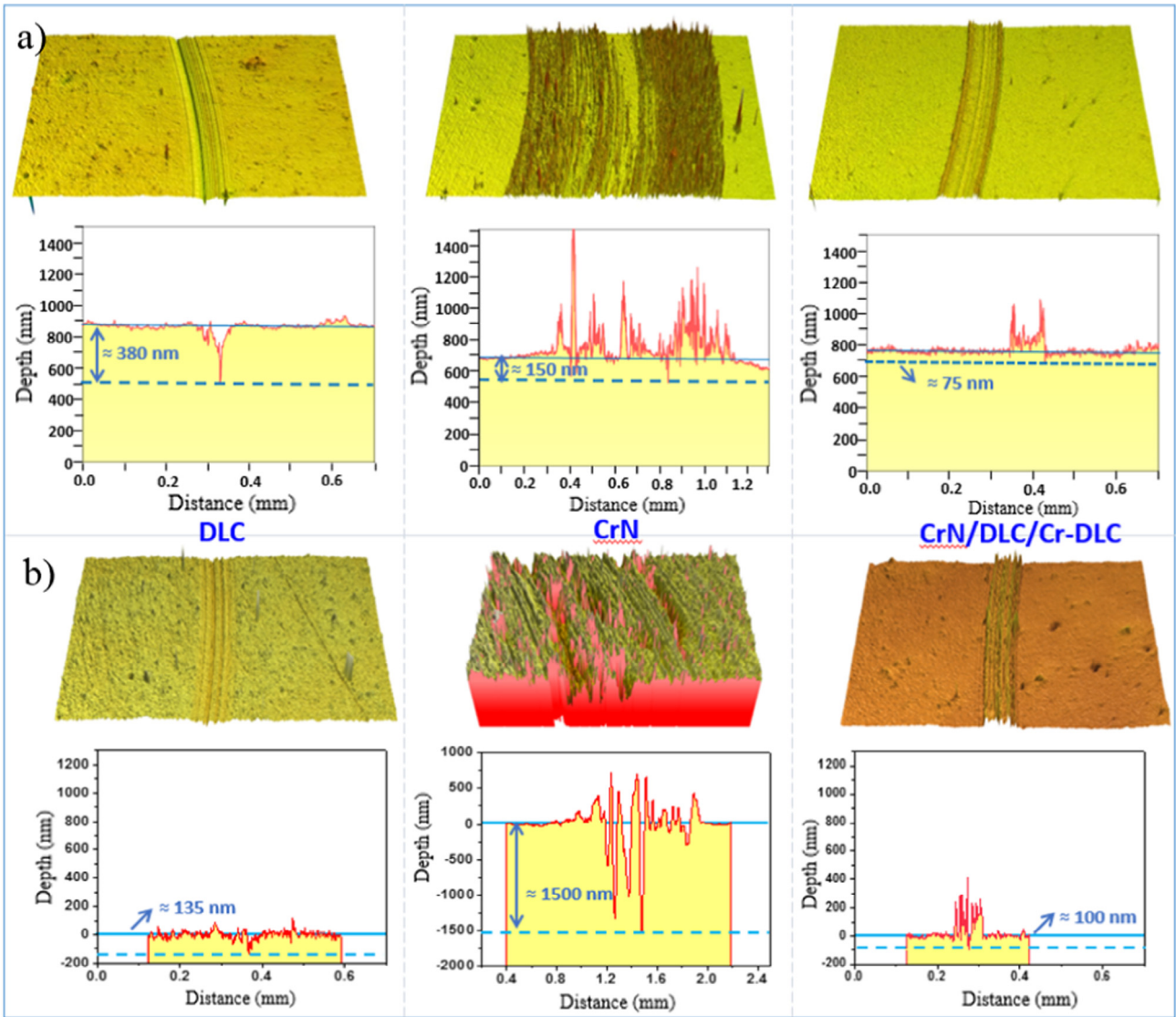


Fig. 8. 3D image and cross sectional profile of wear tracks: (a) sliding with AISI 440C ball and (b) sliding with TC4 ball.

the CrN coating is  $6.2 \times 10^{-16} \text{ m}^3/(\text{N m})$ , which is derived from the depth of wear tracks.

To further understand the wear mechanism of the CrN/DLC/Cr-DLC composite coating, the wear tracks were analysed by SEM and EDS, as shown in Fig. 10 and Table 3. It can be observed from

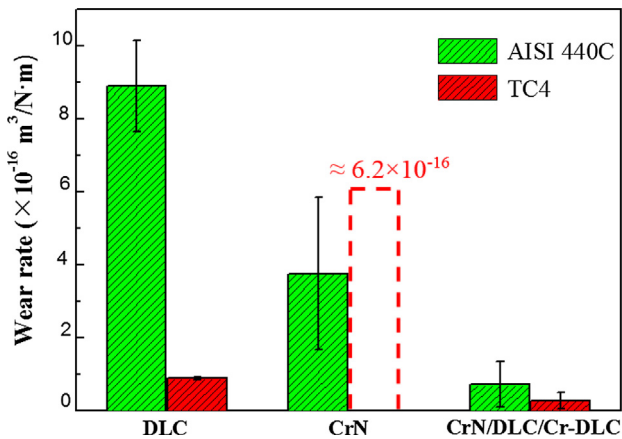
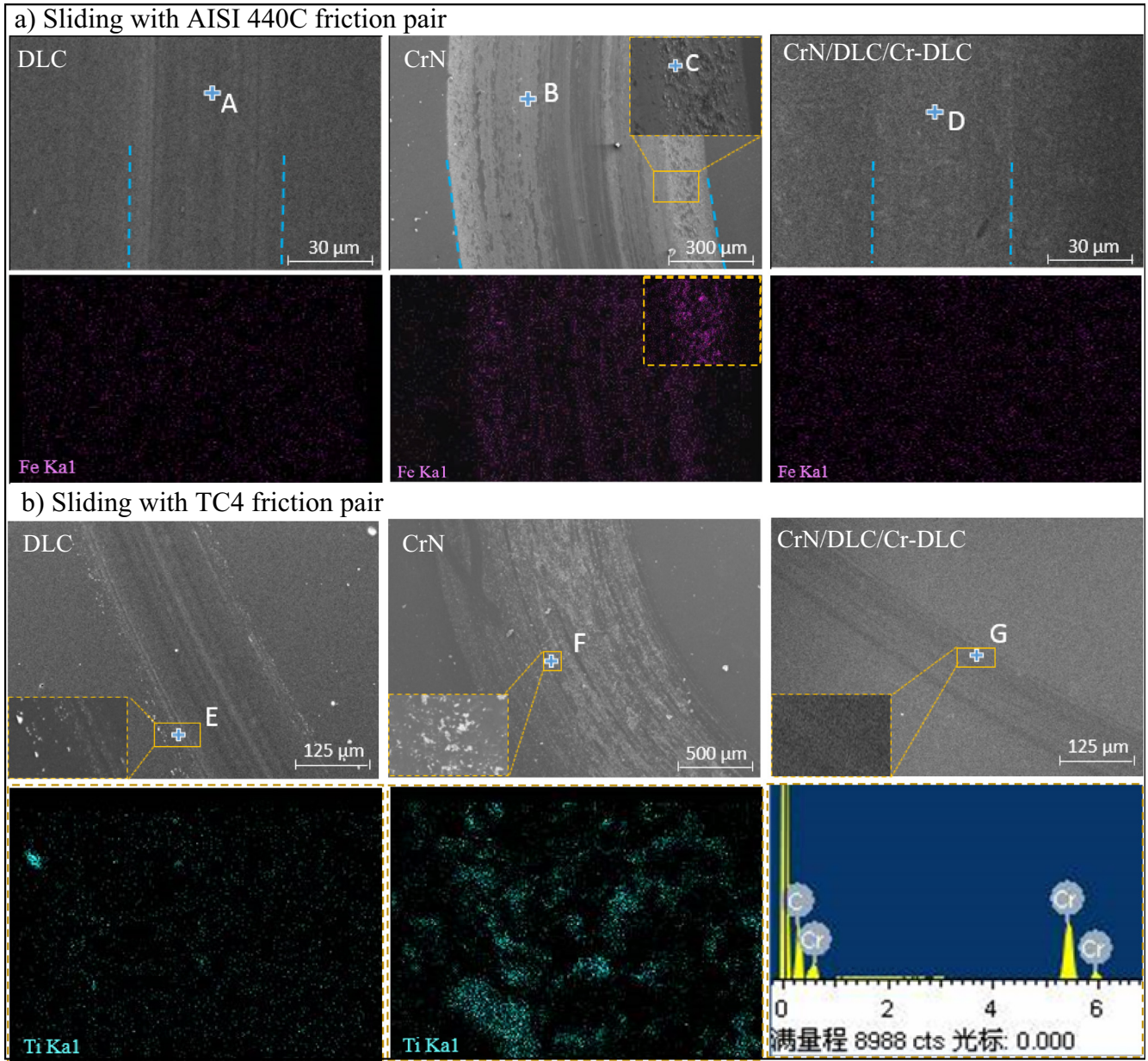


Fig. 9. Wear rate of the deposited coatings.

Fig. 10a that the single DLC coating has a scratched track surface, indicating a groove wear mode. This is consistent with the observed 3D image of the wear track in Fig. 8a. The EDS results (point A) show that a high carbon content on the track surface. According to the previous studies, a lubricating transfer film is usually formed between the amorphous carbon based coating and the friction pair [38]. The single CrN coating has wide wear track with large amount of adhesive bonds along the track, implying an adhesive wear mechanism. The EDS results (points B and C) show that these adhesive bonds mainly contain Cr, Fe, O, Mn, etc., which is similar to the composition of AISI 440C steel. Thus, it can be inferred that an intensive reaction between the CrN coating and the AISI 440C friction pair occurs because of the friction heat. Since the hardness of the CrN coating is higher than that of the AISI 440C friction pair, the wear mainly occurs on the side of friction pair. Therefore, the wear track formed on the surface of the CrN coating is shallow and wide. For the CrN/DLC/Cr-DLC multilayer coating, its wear track is shallow and clean. EDS results show that there is no obvious adhesive bonds on the surface of multilayer coatings.

When the friction pair changes to TC4 ball, the number of the adhesive bonds on the CrN coatings increases. The EDS results (points F) show that these adhesive bonds mainly contain Cr, Ti, Al, O, N, etc. The elements Ti and Al can only come from TC4 ball,





**Fig. 10.** SEM images of wear tracks (top view) and EDS mapping results (bottom view) of the coatings: (a) sliding with AISI 440C ball and (b) sliding with TC4 ball.

which means these welds are surely caused by the bonding between coating and friction pair. Thus it can be inferred that the adhesive wear plays a dominant role in CrN coatings. However, there is no obvious adhesive bonds appears on the surface of the CrN/DLC/Cr-DLC coating. EDS results (point G) also did not detect Ti element. Therefore the adhesive wear resistance of the CrN/DLC/Cr-DLC coating can also be improved when rubbed with highly viscous materials.

In summary, the wear mechanism of as-deposited coatings was simplified in Fig. 11. The excellent tribological property of the multilayer coating can be explained by the following three aspects: Firstly, the existence of amorphous carbon based coatings can act as lubrication layer in a multilayer coating, which can diminish adhesive wear by forming a lubrication transfer layer between the coating and friction pair. Secondly, the CrN layers can act as a hard support layer in a multilayer structure, which can reduce

**Table 3**  
EDS results of the different coatings after friction and wear test.

Point	Cr (at.%)	Fe (at.%)	Mn (at.%)	Ti (at.%)	Al (at.%)	C (at.%)	N (at.%)	O (at.%)
A	29.02	0.84	0.74	–	–	69.40	–	–
B	65.67	5.94	1.59	–	–	2.53	10.34	13.93
C	34.05	25.34	1.04	–	–	3.62	–	35.95
D	50.80	3.62	1.56	–	–	44.01	–	–
E	10.49	–	–	0.14	–	89.38	–	–
F	31.55	0.60	1.17	6.27	1.34	–	38.28	20.79
G	25.86	–	–	–	–	74.14	–	–

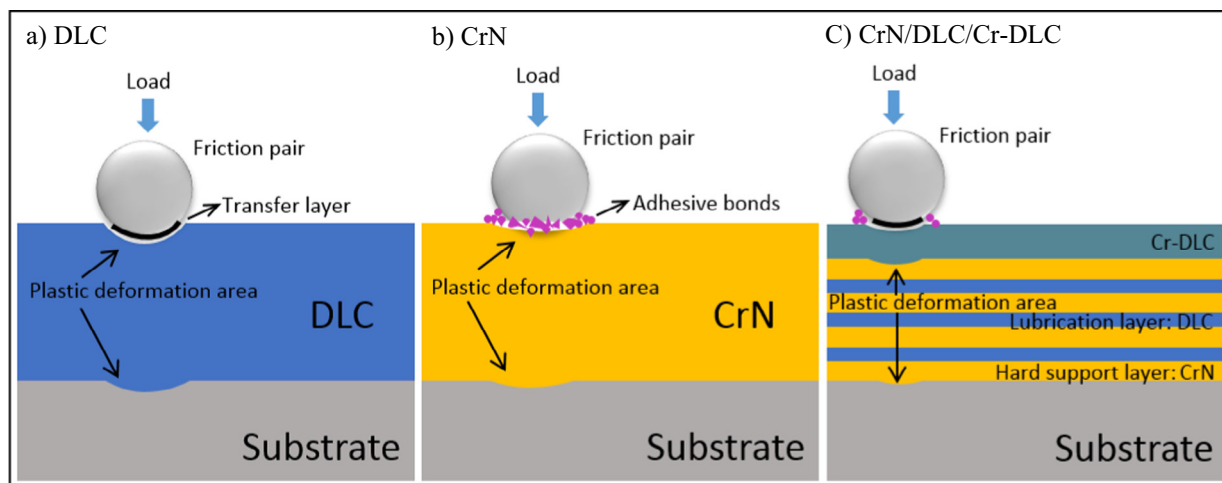


Fig. 11. Schematic diagrams of wear mechanism of the coatings: (a) DLC, (b) CrN, and (c) CrN/DLC/Cr-DLC.

the wear depth by increasing the bearing capacity of vertical loading [39]. Finally, the crack propagation inhibition caused by multilayer design can result in an increase in the fracture toughness. Also the increased elastic recovery in a multilayer structure can improve the coating toughness by decreasing the plastic deformation area [23,36].

#### 4. Conclusions

In conclusion, we developed the CrN/DLC/Cr-DLC multilayer coatings on PECVD device with CFUBMSIP technique in this study. The resultant multilayer coatings consisted of lubricant amorphous carbon based layers and hard transition metal nitride layers. The friction and wear test revealed that the friction coefficient of the CrN/DLC/Cr-DLC multilayer coating can decrease about more than seven times compared with the single CrN coatings. The decrease friction coefficient could help to reduce the adhesive wear of the multilayer coatings. Compared with the single CrN and DLC coating, the wear rate of the CrN/DLC/Cr-DLC multilayer coating is reduced by an order of magnitude to  $7.10 \times 10^{-17}$  (sliding with AISI 440C) and  $2.64 \times 10^{-17}$  (sliding with TC4)  $\text{m}^3/(\text{N m})$ . The low wear rate of multilayer coatings can be contribute to the introduction of lubricant DLC and hard support CrN layers. Also, the enhancement of crack propagation inhibition and increased elastic recovery capability through multilayer design can improve the tribological performance of the CrN/DLC/Cr-DLC multilayer coating. In a word, the CrN/DLC/Cr-DLC multilayer coating prepared in this work own a low wear rate with excellent lubricant and anti-adhesive wear effects. That provides a promising application for various advanced tribological industry.

#### Acknowledgments

The authors gratefully acknowledge the financial support of the National Key Basic Research Program of China (No. 2013CB632302) and the National Natural Science Foundation of China (Nos. 51375471 and 51505465).

#### References

- [1] J. Davim, *Machining of Titanium Alloy*, Springer, 2014, pp. 2–4.
- [2] S. Dolinšek, B. Šuštaršič, J. Kopač, Wear mechanisms of cutting tools in high-speed cutting processes, *Wear* 250 (2001) 349–356.
- [3] Z.Q. Liu, Q.L. An, J.Y. Xu, M. Chen, S. Han, Wear performance of (nc-AlTiN)/(a-Si<sub>3</sub>N<sub>4</sub>) coating and (nc-AlCrN)/(a-Si<sub>3</sub>N<sub>4</sub>) coating in high-speed machining of titanium alloys under dry and minimum quantity lubrication (MQL) conditions, *Wear* 305 (2013) 249–259.
- [4] C.H. Lauro, L.C. Brandao, T.H. Panzera, J.P. Davim, Surface integrity in the micromachining: a review, *Rev. Adv. Mater. Sci.* 40 (2015) 227–234.
- [5] A. Biksa, K. Yamamoto, G. Dosbaeva, S.C. Veldhuis, G.S. Fox-Rabinovich, A. Elfizy, T. Wagg, L.S. Shuster, Wear behavior of adaptive nano-multilayered AlTiN/MexN PVD coatings during machining of aerospace alloys, *Tribol. Int.* 43 (2010) 1491–1499.
- [6] M. Nouari, A. Ginting, Wear characteristics and performance of multi-layer CVD-coated alloyed carbide tool in dry end milling of titanium alloy, *Surf. Coat. Technol.* 200 (2006) 5663–5676.
- [7] H.C. Barshilia, M. Ghosh, R. Shashidhara, K.S. Rajam Ramakrishna, Deposition and characterization of TiAlSiN nanocomposite coatings prepared by reactive pulsed direct current unbalanced magnetron sputtering, *Appl. Surf. Sci.* 256 (2010) 6420–6426.
- [8] M. Kot, L. Majorb, K. Chronowska-Przywara, J.M. Lackner, W. Waldhauser, W. Rakowska, The advantages of incorporating Cr<sub>3</sub>C nanograins into an a-C: H matrix in tribological coatings, *Mater. Des.* 56 (2014) 981–989.
- [9] C.M. Koller, R. Hollerweger, Thermal stability and oxidation resistance of arc evaporated TiAlN, TaAlN, TiAlTaN, and TiAlN/TaAlN coatings, *Surf. Coat. Technol.* 259 (2014) 599–607.
- [10] X.D. Sui, G.J. Li, X.S. Qin, H.D. Yu, X.K. Zhou, K. Wang, Q. Wang, Relationship of microstructure, mechanical properties and titanium cutting performance of TiAlN/TiAlSiN composite coated tool, *Ceram. Int.* 42 (2016) 7524–7532.
- [11] L. Chen, J. Paulitsch, Y. Du, P.H. Mayrhofer, Thermal stability and oxidation resistance of Ti–Al–N coatings, *Surf. Coat. Technol.* 206 (2012) 2954–2960.
- [12] J. Musil, Hard and superhard nanocomposite coatings, *Surf. Coat. Technol.* 125 (2000) 322–330.
- [13] J.F. Wu, N.R. He, H.X. Li, X.H. Liu, L. Ji, X.P. Huang, J.M. Chen, Deposition and characterization of TiAlSiN coatings prepared by hybrid PVD coating system, *Surf. Interface Anal.* 47 (2015) 184–191.
- [14] T. Shimizu, Y. Teranishi, K. Morikawa, H. Komiya, T. Watanabe, H. Nagasaka, M. Yang, Impact of pulse duration in high power impulse magnetron sputtering on the low-temperature growth of wurtzite phase (Ti, Al)N films with high hardness, *Thin. Solid. Films* 581 (2015) 39–47.
- [15] X.C. Li, P.L. Ke, X.C. Liu, A.Y. Wang, Discharge characteristics of Ti and film preparation using hybrid high power impulse magnetron sputtering, *Acta Metall. Sin.* 50 (2014) 879.
- [16] Y.X. Qiu, S. Zhang, J.W. Lee, B. Li, Y.X. Wang, D.L. Zhao, Self-lubricating CrAlN/VN multilayer coatings at room temperature, *Appl. Surf. Sci.* 279 (2013) 189–196.
- [17] T. Wang, G.J. Zhang, B.L. Jiang, Microstructure, mechanical and tribological properties of TiMoN/Si<sub>3</sub>N<sub>4</sub> nano-multilayer films deposited by magnetron sputtering, *Appl. Surf. Sci.* 326 (2015) 162–167.
- [18] H. Yamaguchi, A.K. Srivastava, M.A. Tan, Magnetic abrasive finishing of cutting tools for machining of titanium alloys, *CIRP Ann-Manuf. Technol.* 61 (2012) 311–314.
- [19] J. Robertson, Diamond-like amorphous carbon, *Mat. Sci. Eng. R* 37 (2002) 129–281.
- [20] X.Q. Liu, J. Yang, J.Y. Hao, J.Y. Zheng, Q.Y. Gong, W.M. Liu, A near-frictionless and extremely elastic hydrogenated amorphous carbon film with self-assembled dual nanostructure, *Adv. Mater.* 24 (2012) 4614–4617.
- [21] J.J. Wang, J.B. Pu, G.G. Zhang, L.P. Wang, Interface architecture for superthick carbon-based films toward low internal stress and ultrahigh load-bearing capacity, *ACS Appl. Mater. Inter.* 5 (2013) 5015–5024.
- [22] A. Erdemir, C. Donnet, Tribology of diamond-like carbon films: recent progress and future prospects, *J. Phys. D: Appl. Phys.* 39 (2006) 311–327.
- [23] J.Y. Zhang, G. Liu, X. Zhang, G.J. Zhang, J. Sun, E. Ma, A maximum in ductility and fracture toughness in nanostructured Cu/Cr multilayer films, *Scripta Mater.* 62 (2010) 333–336.
- [24] S. Kaciulis, A. Mezzi, G. Montesperelli, F. Lamastra, M. Rapone, F. Casadei, T. Valente, G. Gusmano, Multi-technique study of corrosion resistant CrN/Cr/CrN and CrN: C coatings, *Surf. Coat. Technol.* 201 (2006) 313–319.



- [25] R. Ali, M. Sebastiani, E. Bemporad, Influence of Ti–TiN multilayer PVD-coatings design on residual stresses and adhesion, *Mater. Des.* 75 (2015) 47–56.
- [26] J.H. Lee, W.M. Kim, T.S. Lee, M.K. Chung, B.K. Cheong, S.G. Kim, Mechanical and adhesion properties of Al/AlN multilayered thin films, *Surf. Coat. Technol.* 220 (2000) 133–134.
- [27] M. Kot, Ł. Major, J. Lackner, The tribological phenomena of a new type of TiN/a-C:H multilayer coatings, *Mater. Design* 51 (2013) 280–286.
- [28] D.W. Kim, K.W. Kim, Tribological characteristics of Cr/CrN/a-C:H/W/a-C:H coating under boundary lubrication conditions with glycerol mono-oleate (GMO) and molybdenum dithiocarbamate (MoDTC), *Wear* 342–343 (2015) 107–116.
- [29] J.Y. Zheng, X.D. Ren, J.Y. Hao, A. Li, W.M. Liu, Carbon nanostructures as attractive toughening and lubricant agents in TiN porous films, *Appl. Surf. Sci.* 393 (2017) 60–66.
- [30] A. Ferrari, J. Robertson, Interpretation of Raman spectra of disordered and amorphous carbon, *Phys. Rev. B* 61 (2000) 14095–14107.
- [31] L.L. Sun, P. Guo, P.L. Ke, X.W. Li, A.Y. Wang, Synergistic effect of Cu/Cr co-doping on the wettability and mechanical properties of diamond-like carbon films, *Diam. Relate. Mater.* 68 (2016) 1–9.
- [32] A. Modabberasl, P. Kameli, M. Ranjbar, H. Salamati, R. Ashiri, Fabrication of DLC thin films with improved diamond-like carbon character by the application of external magnetic field, *Carbon* 94 (2015) 485–493.
- [33] C. Forsich, D. Heim, T. Mueller, Influence of the deposition temperature on mechanical and tribological properties of a-C:H: Si coatings on nitrated and postoxidized steel deposited by DC-PACVD, *Surf. Coat. Technol.* 203 (2008) 521–525.
- [34] M. Tabbal, P. Merel, M. Chaker, M.A. El Khakani, E.G. Herbert, B.N. Lucas, M.E. O'Hern, Effect of laser intensity on the microstructural and mechanical properties of pulsed laser deposited diamond-like-carbon thin films, *J. Appl. Phys.* 85 (1999) 3860–3865.
- [35] P.K.P. Rupa, P.C. Chakraborti, S.K. Mishra, Structure and indentation behavior of nanocomposite Ti-B-N films, *Thin. Solid. Films* 564 (2014) 160–169.
- [36] C.Q. Guo, Z.L. Pei, D. Fan, J. Gong, C. Sun, Microstructure and tribomechanical properties of (Cr, N)-DLC/DLC multilayer films deposited by a combination of filtered and direct cathodic vacuum arcs, *Diam. Relate. Mater.* 60 (2015) 66–74.
- [37] W. Dai, J.M. Liu, D.S. Geng, P. Guo, J. Zheng, Q.M. Wang, Microstructure and property of diamond-like carbon films with Al and Cr co-doping deposited using a hybrid beams system, *Appl. Surf. Sci.* 388 (2016) 503–509.
- [38] T.W. Scharf, I.L. Singer, Quantification of the thickness of carbon transfer films using Raman Tribometry, *Tribol. Lett.* 14 (2003) 137–145.
- [39] S.G. Ma, D.Y. Yu, H.W. Yang, Y.C. Zhang, Properties of Cr+Ti+TiNC/TiNC+DLC films prepared by composite ion plating, *Nucl. Technol.* 31 (2008) 111–114.